Supp. Figure 1. Hedrick

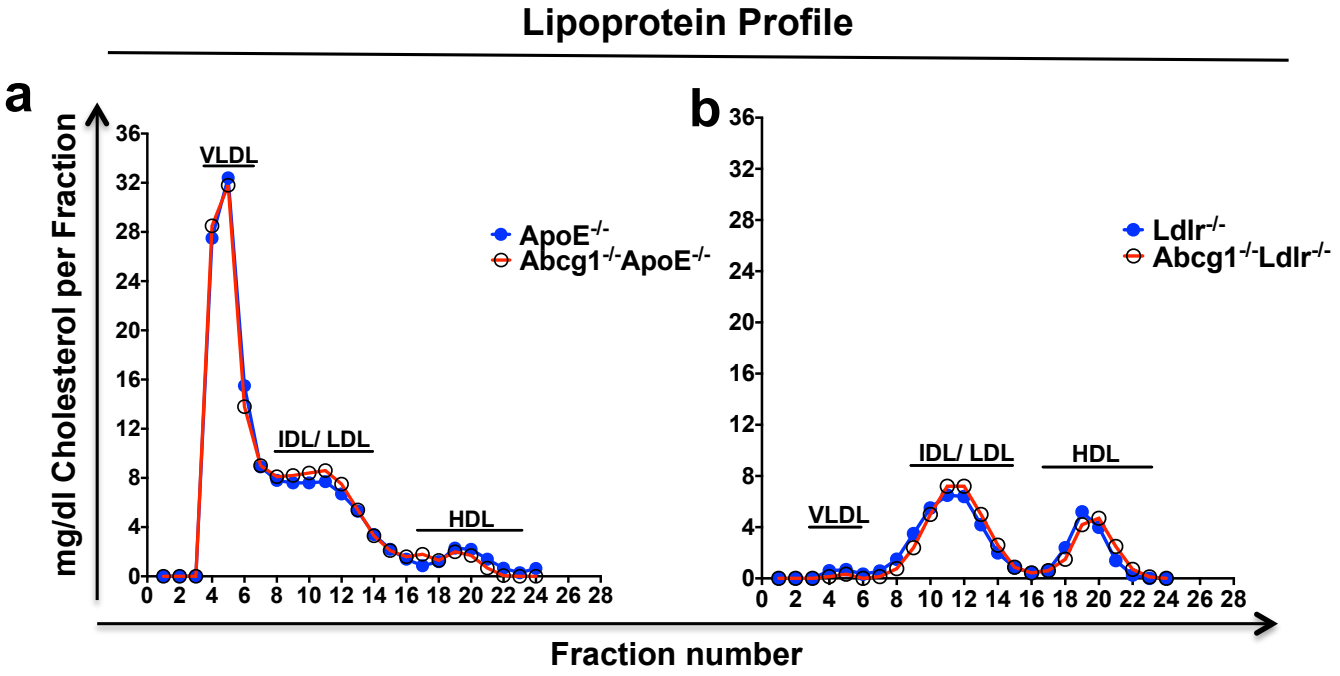

Supplementary Figure 1
The loss of ABCG1 does not change plasma lipoprotein profiles in tumor-bearing hypercholesterolemic mice. Chow diet-fed (**a**) *ApoE*$^{-/-}$*, Abcg1*$^{-/-}$ *ApoE*$^{-/-}$ and (**b**) *Ldlr*$^{-/-}$*, Abcg1*$^{-/-}$*Ldlr*$^{-/-}$ mice were injected with MB49 tumor cells. 12 days later, blood plasma from 5 tumor-bearing mice for each group was pooled and lipoprotein profiles were analyzed by FPLC. Graph shows VLDL, IDL/LDL and HDL levels in all groups.

Supp. Figure 2. Hedrick

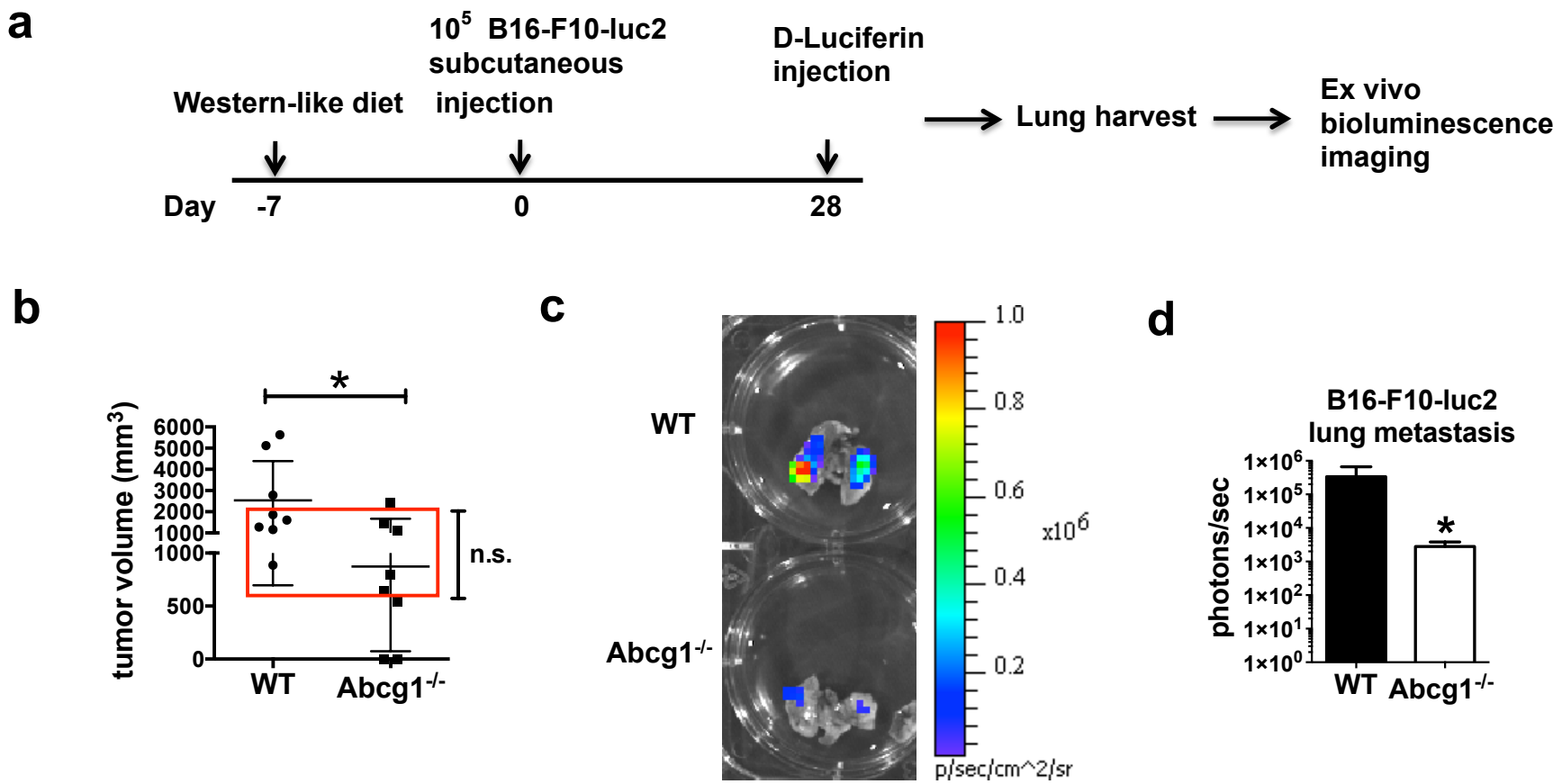

Supplementary Figure 2

***Abcg1*$^{-/-}$ mice on Western-like diet show decreased tumor metastasis.** (**a-d**) Lung metastasis was quantified based on luminescence detected by using IVIS 200 Bioluminescence imager.(**a**) Schematic diagram of the experimental design is shown. (**b**) The graph shows tumor volume in Western-like diet-fed *Abcg1*$^{-/-}$ and WT mice 28 days after injection of B16-F10-luc2 cells subcutaneously. Red box shows the mice that were picked for the spontaneous metastasis analysis. *p<0.05, n.s.: not significant, two tailed Student's t test (**c**) Representative lung images and (**d**) Bar graph show spontaneous B16-F10-luc2 lung metastasis in *Abcg1*$^{-/-}$ (*n*=5) and WT (*n*=5) mice. Data is pooled from 2 independent experiments with similar results. (mean ± s.e.m., *P< 0.05, Wilcoxon-matched-pairs signed rank test)

Supp. Figure 3. Hedrick

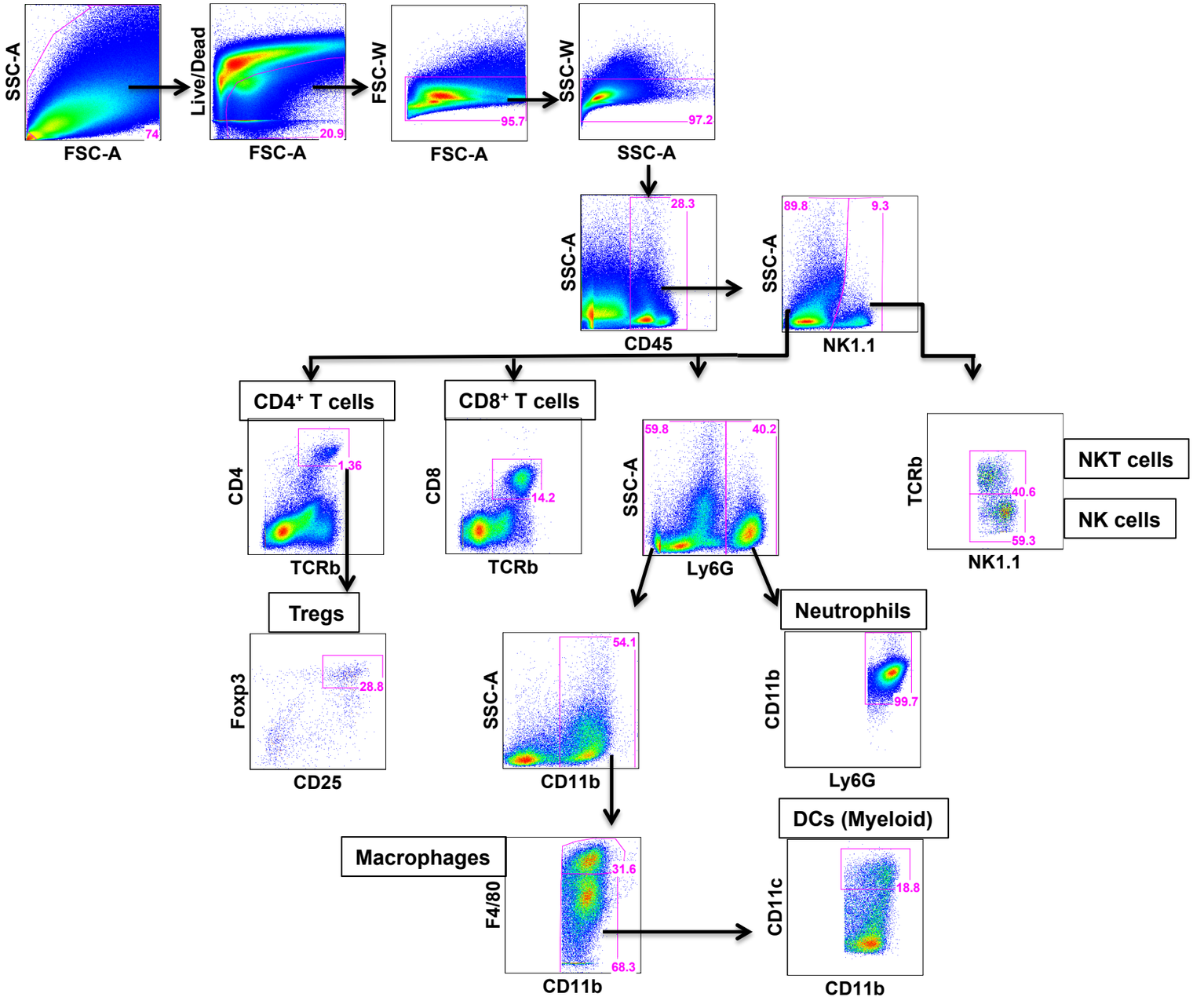

Supplementary Figure 3
Flow cytometry gating strategy to identify immune cell subsets in the tumor. Single-cell suspension from tumor was stained with different fluorophore-conjugated antibodies and analyzed by flow cytometry. Among single cells, the live cells, singlets and CD45$^+$ cells were selected for further analysis to identify NKT cells (NK1.1$^+$, TCRβ$^+$), NK cells (NK1.1$^+$, TCRβ$^-$), CD4$^+$ T cells (NK1.1$^-$, TCRβ$^+$, CD4$^+$), CD8$^+$ T cells (NK1.1$^-$, TCRβ$^+$ CD8$^+$), Tregs (NK1.1$^-$, TCRβ$^+$, CD4$^+$,CD25$^+$, Foxp3$^+$), neutrophils (NK1.1$^-$, Ly6G$^+$, CD11b$^+$), macrophages (NK1.1$^-$, Ly6G$^-$, CD11b$^+$, F4/80^{high}) and myeloid dendritic cells (NK1.1$^-$, Ly6G$^-$, F4/80$^-$, CD11b$^+$ CD11c$^+$).

Supp. Figure 4. Hedrick

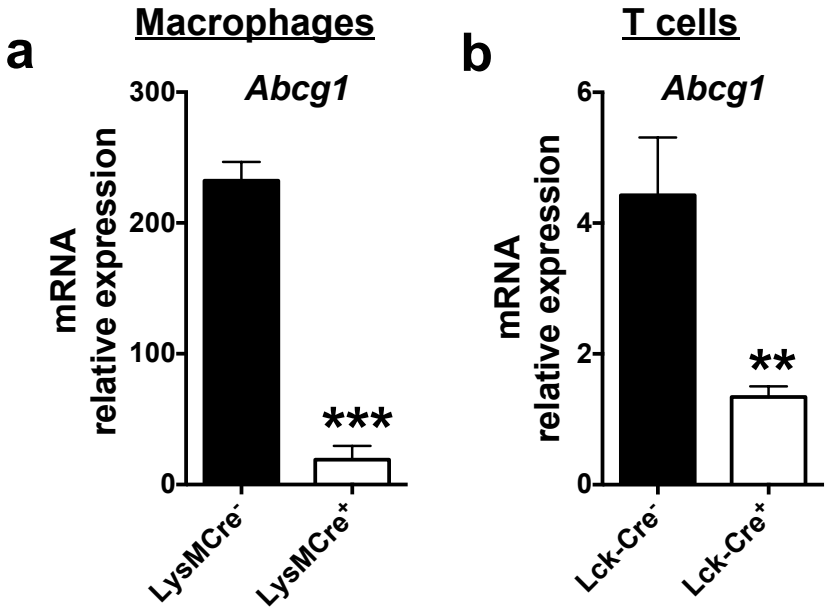

Supplementary Figure 4
Deletion of ABCG1 in macrophages from *Abcg1*$^{fl/fl}$-LysM-Cre^{+} mice and T cells from *Abcg1*$^{fl/fl}$-Lck-Cre^{+} mice.
(**a**) Macrophages were FACS-sorted from peritoneal lavage of *Abcg1*$^{fl/fl}$-LysM-Cre^{-} and *Abcg1*$^{fl/fl}$-LysM-Cre^{+} mice. (**b**) T cells were FACS-sorted from spleen of *Abcg1*$^{fl/fl}$-Lck-Cre^{-} and *Abcg1*$^{fl/fl}$-Lck-Cre^{+} mice. Expression of *Abcg1* was assessed by qPCR. (mean ± s.e.m., $^{**}P < 0.01$, $^{***}P < 0.001$, two-tailed Student's t test).

Supp. Figure 5. Hedrick

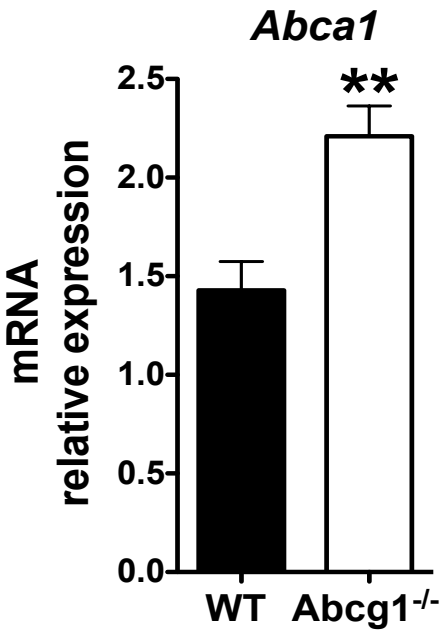

Supplementary Figure 5
ABCG1-deficient tumor macrophages display increased expression of *Abca1*. Macrophages were FACS-sorted from tumors from Western-like diet-fed *Abcg1*$^{-/-}$ (*n*=6) and WT (*n*=6) mice 20 days after inoculation of MB49 cells. Expression of *Abca1* was measured by qPCR. Data are pooled from 2 independent experiments with similar results. (mean ± s.e.m., $^{**}P < 0.01$, two-tailed Student's t test).

Supp. Figure 6. Hedrick

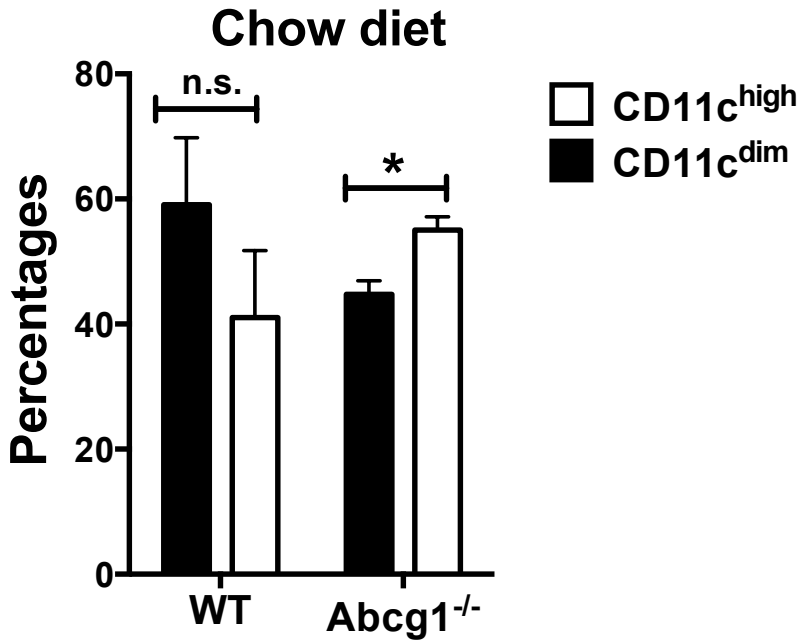

Supplementary Figure 6
Chow diet-fed *Abcg1*$^{-/-}$ mice display a slightly higher percentage of CD11c^{high} (M1-like) macrophages in the tumor. Tumor cells from Western diet-fed *Abcg1*$^{-/-}$ (*n*=3) and WT mice (*n*=3) mice were analyzed by flow cytometry 20 days after injection of MB49 cells. Bar graph shows percentages of CD11c^{high} (M1-like) and CD11c^{dim} (M2-like) macrophages (CD45^{+}, NK1.1^{-}, Ly6G^{-}, CD11b^{+}, F4/80^{high}) in the tumor. Data is representative of 2 independent experiments with similar results (mean ± s.e.m., $^{*}P < 0.05$, two-tailed Student's t test).

Supp. Figure 7. Hedrick

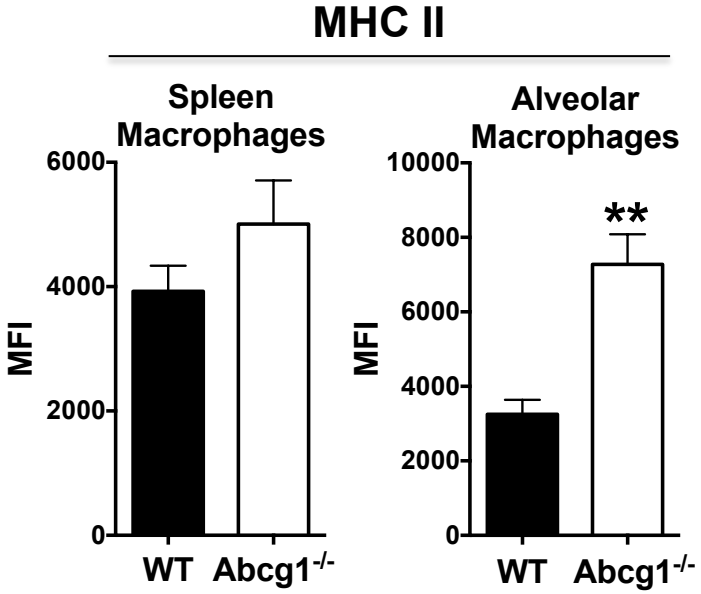

Supplementary Figure 7
Alveolar macrophages in Western-like diet-fed tumor-bearing *Abcg1*$^{-/-}$ mice display an M1 bias.
Spleen and lung cells from Western-like diet-fed *Abcg1*$^{-/-}$ (*n*=5) and WT mice (*n*=5) mice were analyzed by flow cytometry 20 days after injection of MB49 cells. Bar graphs show the MFI of MHC II on spleen macrophages ($CD19^-$,$NK1.1^-$, $Ly6G^-$, $CD11b^+$, $F4/80^+$) (left) and alveolar macrophages ($CD45^+$, $CD19^-$, $NK1.1^-$, $Ly6G^-$, $CD11c^+$, $SiglecF^+$) (right). Data are representative of 2 independent experiments with similar results (mean ± s.e.m., $^{**}P < 0.01$, two-tailed Student's t test).

Supp. Figure 8.Hedrick

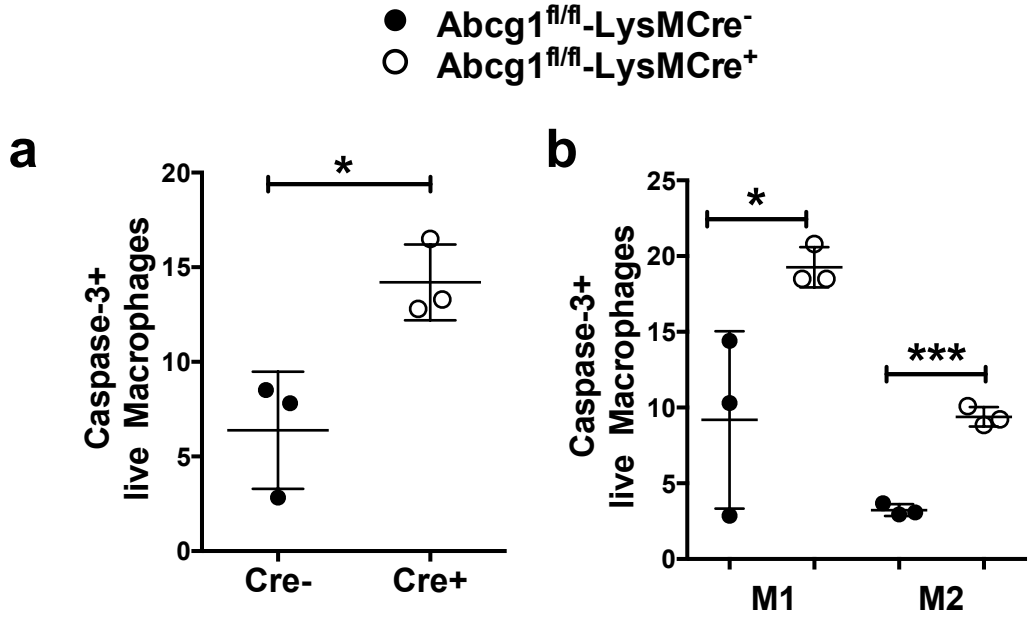

Supplementary Figure 8

ABCG1-deficient macrophages display enhanced apoptosis in the tumor. Tumor cells from Western-like diet-fed *Abcg1*$^{fl/fl}$-LysM-Cre^{+} (n=3) and *Abcg1*$^{fl/fl}$-LysM-Cre^{-} (n=3) mice were analyzed for apoptosis by Caspase-3 staining and flow cytometry 12 days after injection of MB49 cells. Dot plot show percentages of apoptotic (Caspase-3^{+} live) (**a**) total macrophages and (**b**) M1 (CD11c^{high}) and M2 (CD11c^{dim}) macrophages in the tumor. Data are representative of 2 independent experiments with similar results (mean ± s.e.m., *$P < 0.05$ ***$P < 0.001$, two-tailed Student's t test).

Supp. Figure 9. Hedrick

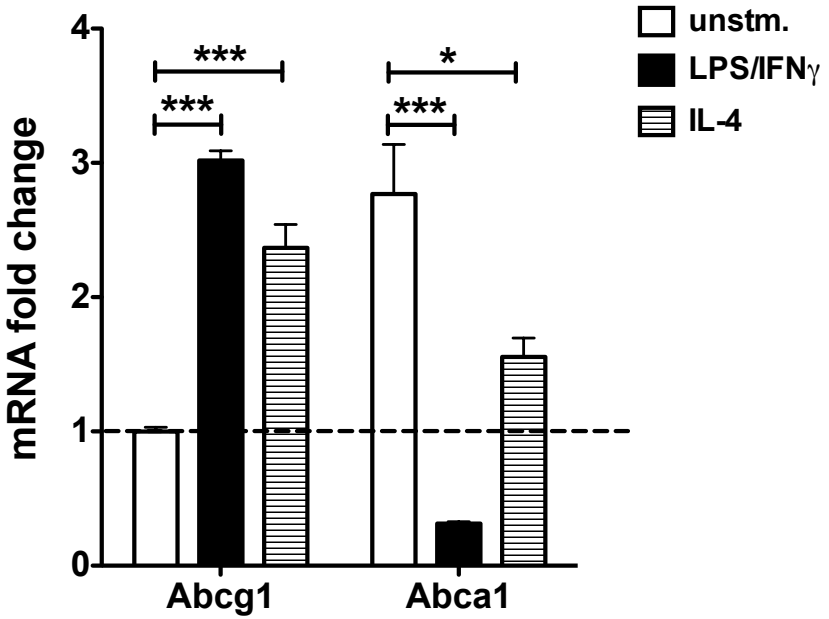

Supplementary Figure 9
Polarized WT macrophages exhibit enhanced ABCG1 and reduced ABCA1 expression. WT bone marrow-derived macrophages were polarized to an M1 phenotype by IFNγ/LPS stimulation or to an M2 phenotype by IL-4 stimulation, *in vitro.* Expression of *Abcg1* and *Abca1* was assessed by qPCR. Data are representative of 2 independent experiments with similar results (mean ± s.e.m., $*P < 0.05$, $***P < 0.001$, two-tailed Student's t test).